PNAS

Supplementary Information for

Fin ray branching is defined by TRAP$^+$ osteolytic tubules in zebrafish

João Cardeira-da-Silva[a,b,c,1,2], Anabela Bensimon-Brito[a,b,d,2], Marco Tarasco[a,c], Ana S. Brandão[e], Joana T. Rosa[c,4], Jorge Borbinha[e], Paulo J. Almeida[f], António Jacinto[e], M. Leonor Cancela[c,g], Paulo J. Gavaia[c,g,3], Didier Y. R. Stainier[a,b,3], Vincent Laizé[c,1,3]

[a] Department of Developmental Genetics, Max Planck Institute for Heart and Lung Research, 61231 Bad Nauheim, Germany
[b] DZHK – German Centre for Cardiovascular Research, Partner Site Rhine-Main, 61231 Bad Nauheim, Germany
[c] CCMAR – Centre of Marine Sciences, University of Algarve, 8005-139 Faro, Portugal
[d] INSERM – National Institute of Health and Medical Research, Atip-Avenir, Aix Marseille University, Marseille Medical Genetics, 13005 Marseille, France
[e] CEDOC – Chronic Diseases Research Center, NOVA Medical School, NOVA University of Lisbon, 1150-082 Lisbon, Portugal
[f] STAB VIDA – Investigação e Serviços em Ciências Biológicas, Madan Parque, 2825-182 Caparica, Portugal
[g] FMCB – Faculty of Medicine and Biomedical Sciences and ABC – Algarve Biomedical Center, University of Algarve, 8005-139 Faro, Portugal

[1] To whom correspondence may be addressed. E-mail: joao.cardeira-da-silva@mpi-bn.mpg.de or vlaize@ualg.pt
[2] J.C.-d.-S. and A.B.-B. contributed equally to this work
[3] P.J.G., D.Y.R.S and V.L. contributed equally to this work
[4] Present address: S2AQUA – Sustainable and Smart Aquaculture Collaborative Laboratory, 8700-194 Olhão, Portugal

This PDF file includes:

Other supplementary materials for this manuscript include the following:

Movies S1 and S2

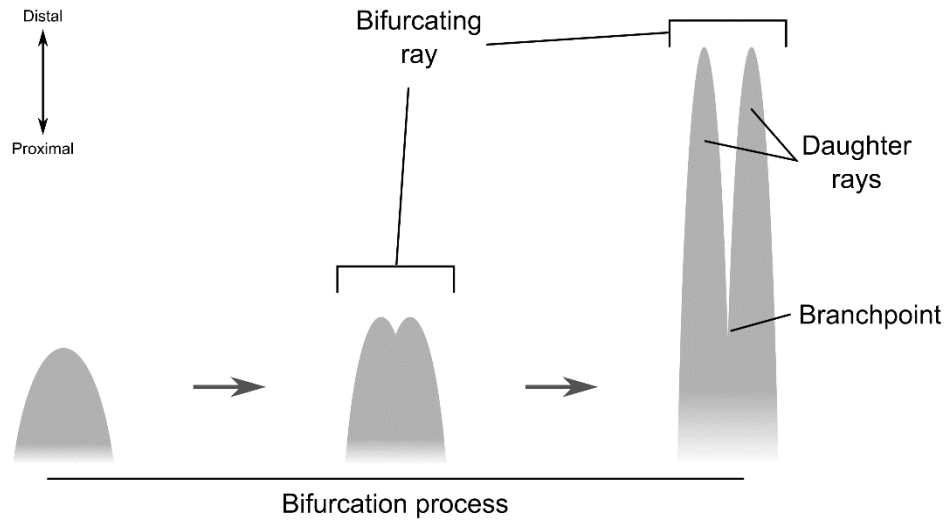

Fig. S1. Simple scheme of the ray bifurcation process. The gray shapes represent the mineralized regenerating bony rays. A bifurcating ray displays two visible daughter rays forming distally. The branchpoint is the most proximal point of daughter ray splitting.

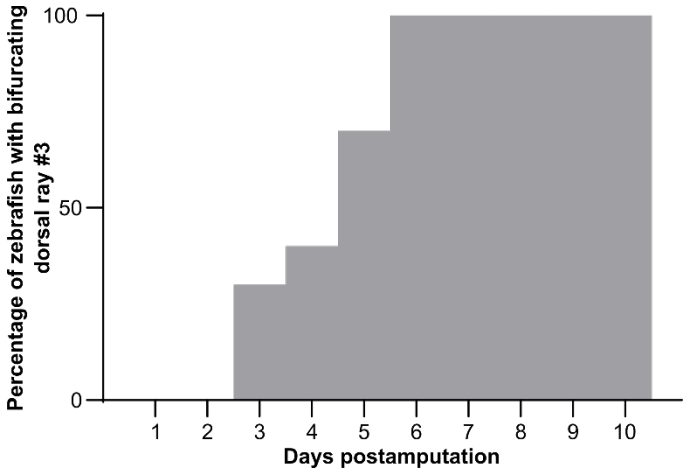

Fig. S2. Percentage of zebrafish (*N* = 10) exhibiting bifurcating dorsal ray #3. Based on the same data as for Fig. 1*B*.

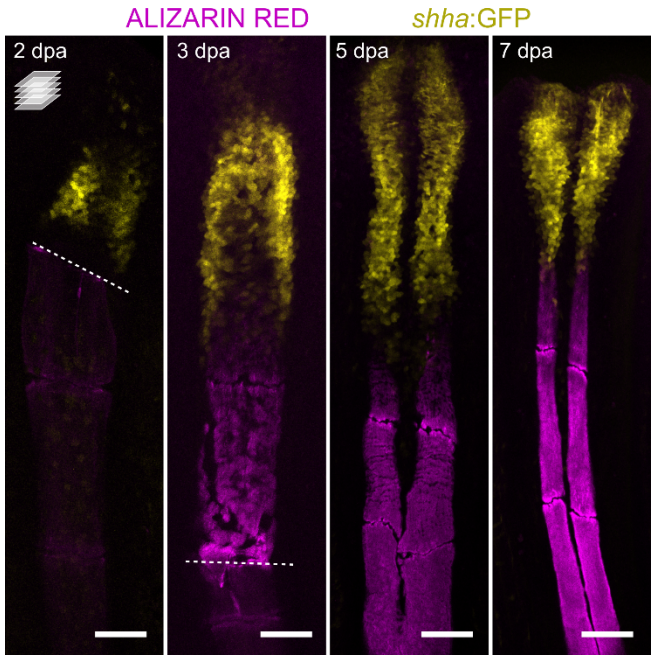

Fig. S3. Confocal images of representative regenerating rays at different time points, showing the segregation of *shha:*GFP^{+} domains (yellow) close to the forming bone (magenta). White dashed lines indicate the amputation plane; amputation planes at 5 and 7 dpa are not included in the pictures. Scale bars: 100 μm.

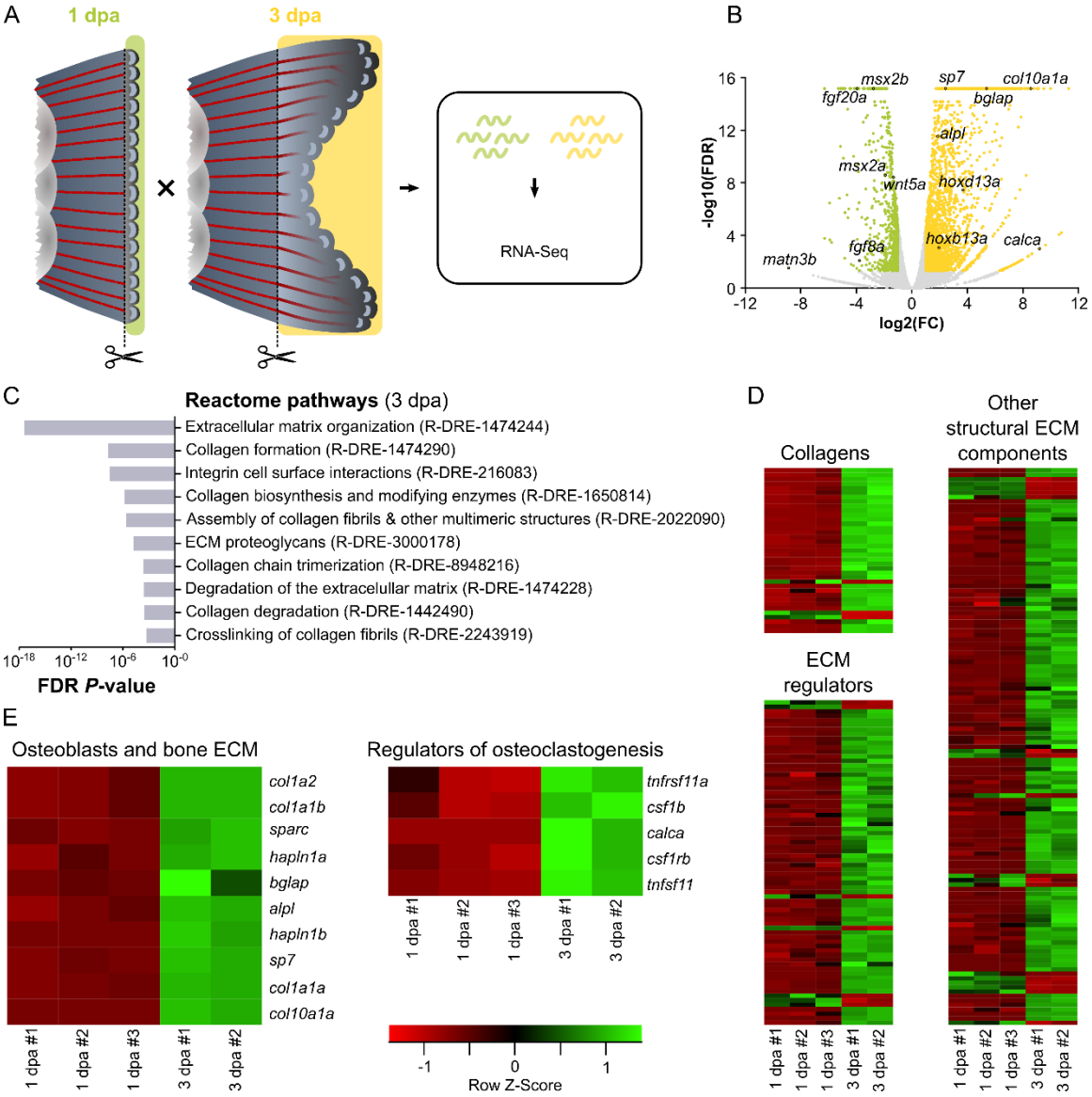

Fig. S4. RNA-Seq analysis reveals the upregulation of osteoblast- and osteoclast-related genes, and the activation of morphogenetic and ECM remodeling processes in regenerates preceding bifurcation. (*A*) Experimental design for RNA-Seq. (*B*) Volcano plot showing differentially expressed genes (FC ≥ 2; FDR < 0.05). Green and yellow represent genes with enriched expression at 1 and 3 dpa, respectively. (*C*) Top 10 overrepresented gene ontology terms, represented by Reactome pathways, among the list of genes upregulated at 3 dpa. (*D*, *E*) Heatmaps for individual samples, showing the relative expression of genes encoding collagens, ECM regulators, and other structural ECM components (*D*), and of osteoblast-specific genes, bone ECM genes, and genes involved in osteoclastogenesis (*E*).

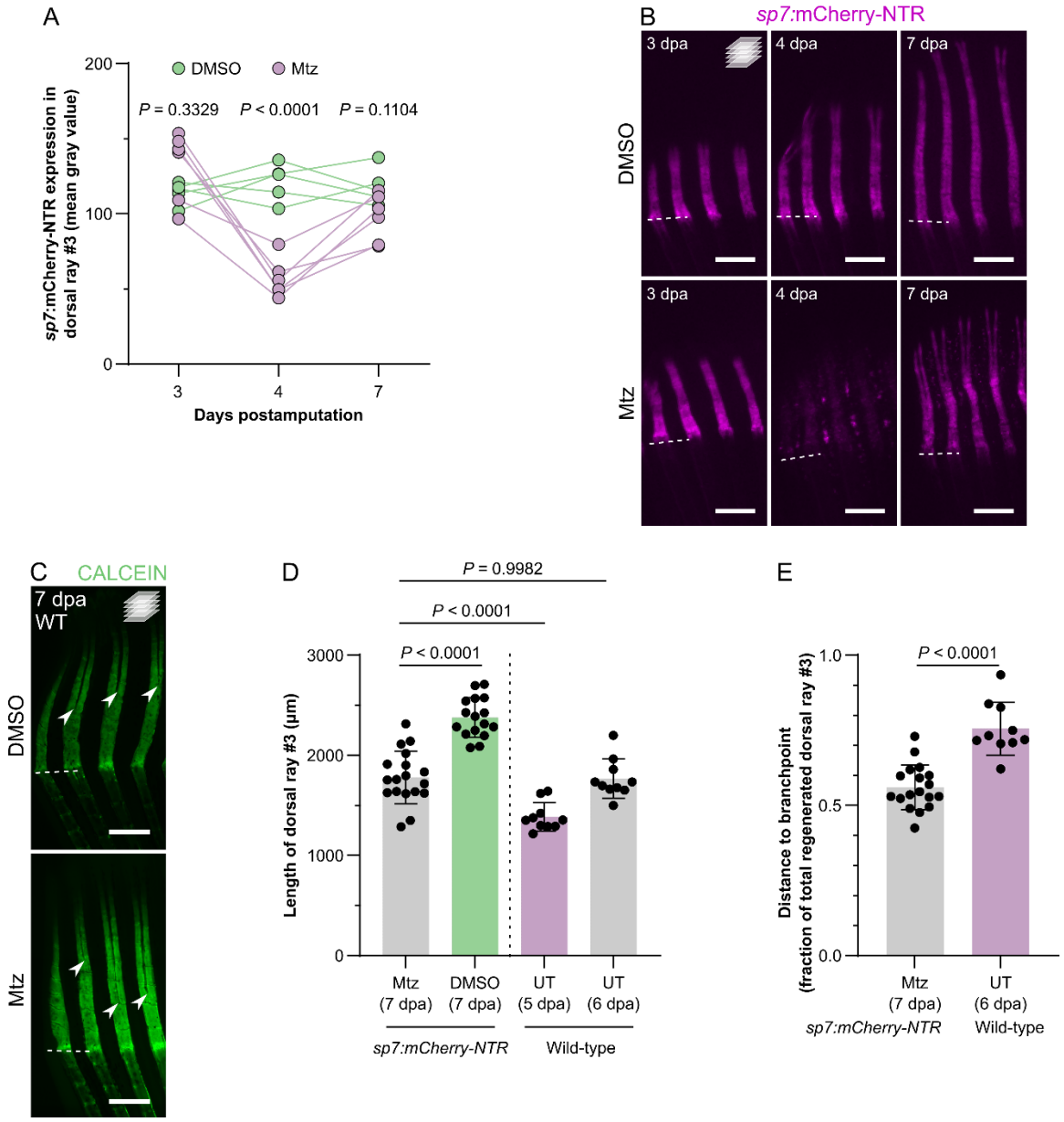

Fig. S5. Validation analyses of the osteoblast ablation studies. (*A*, *B*) Individual quantification (*C*) and stereomicroscope images (*B*) showing a decrease in *sp7:mCherry-NTR* expression (i.e., fluorescence intensity) in regenerating dorsal ray #3 shortly after Mtz exposure (4 dpa), followed by a recovery at a later stage (7 dpa). (*C*) Confocal images representative of fins from wild-type DMSO- and Mtz-treated zebrafish, at 7 dpa. (*D*) Quantification of total length of dorsal ray #3 of Mtz- and DMSO-treated *sp7:mCherry-NTR* transgenic zebrafish at 7 dpa and untreated (UT) wild-type zebrafish at 5 and 6 dpa. These data are a combination of two distinct experiments to compare rays with similar length; wild-type animals analyzed are the same as in Fig. 1*B*. (*E*) Quantification of the branchpoint position in Mtz-treated *sp7:mCherry-NTR* zebrafish at 7 dpa and untreated wild-type zebrafish at 6 dpa (similar ray length). The dots in all graphs represent individual zebrafish; bar graphs show the mean ± SD. Two-way ANOVA ($P < 0.0001$ for time-point × treatment, $P = 0.0014$ for time-point, $P = 0.0007$ for treatment and $P = 0.7787$ for individuals) and Šidák's post hoc test in *A* (*P* values on the graph represent comparison between

treatments); one-way ANOVA ($P < 0.0001$) and Tukey's post hoc test in *D*; two-tailed Student's t-test in *E*. Dashed white lines mark the amputation planes. Scale bars: 500 μm.

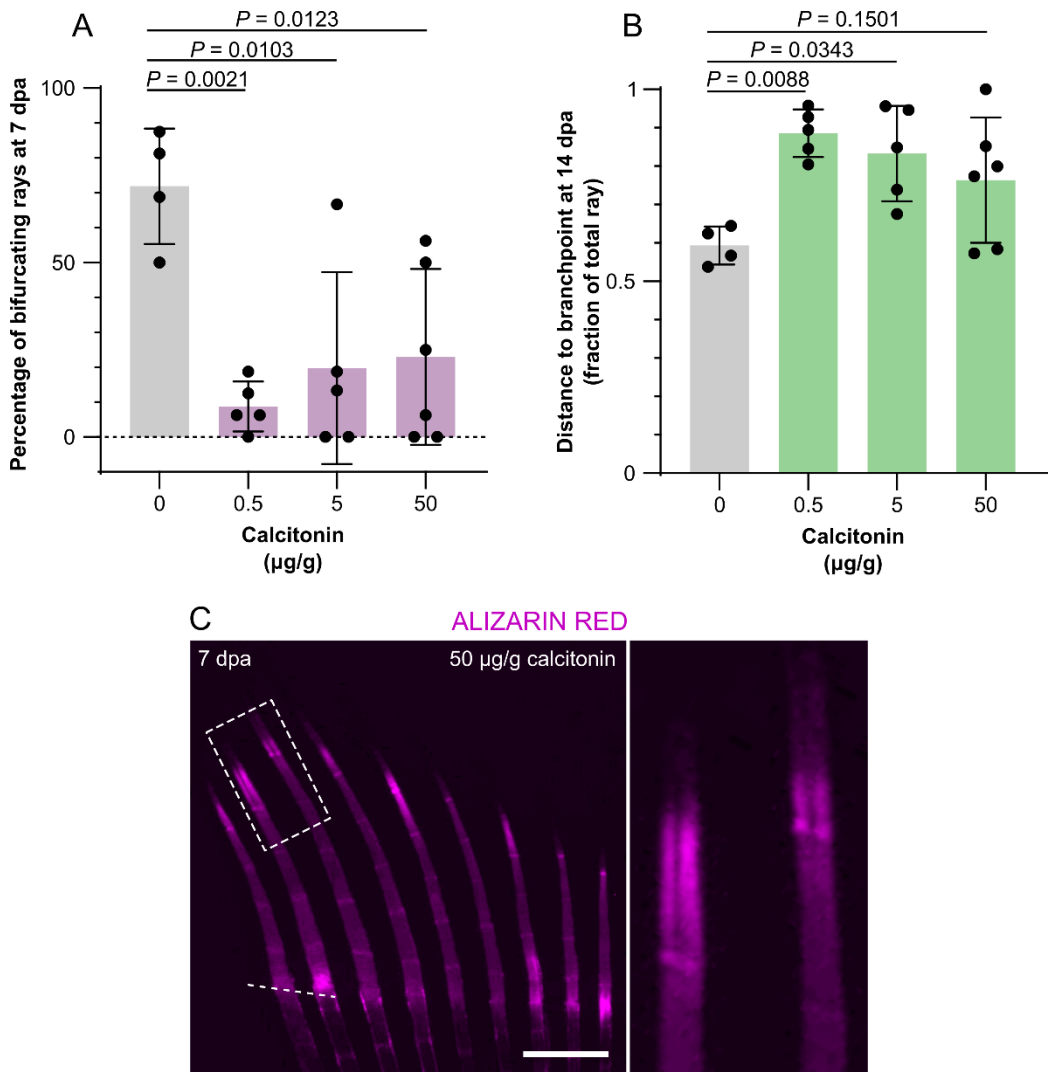

Fig. S6. Additional analyses provide further evidence for a bifurcation phenotype upon osteoclast activity inhibition. (*A*) Quantification of the percentage of bifurcating rays at 7 dpa shows a decrease after calcitonin treatment. (*B*) Relative distance from the amputation plane to the branchpoint at 14 dpa is increased after calcitonin treatment. (*C*) Stereomicroscope image of representative mineralized rays from a fin at a bifurcation stage of zebrafish treated with the highest calcitonin concentration (50 µg/g), showing impaired bifurcation and heterogeneity in mineralization. Dashed white line marks the amputation plane. The dashed rectangle marks the magnified area on the *Right*. All graphs show the mean ± SD. One-way ANOVA ($P = 0.0025$ in *A* and $P = 0.0111$ in *B*) and Tukey's post hoc test. Scale bar: 500 µm.

Table S1. Statistics details on Tukey's multiple comparisons test for the data shown in Fig. 1*B*.

Tukey's multiple comparisons test	Summary	Adjusted *P* Value
3 dpa vs. 4 dpa	Nonsignificant	0.4099
3 dpa vs. 5 dpa	Nonsignificant	0.1575
3 dpa vs. 6 dpa	Nonsignificant	0.0782
3 dpa vs. 7 dpa	*	0.0461
3 dpa vs. 8 dpa	*	0.0474
3 dpa vs. 9 dpa	*	0.0247
3 dpa vs. 10 dpa	Nonsignificant	0.0512
4 dpa vs. 5 dpa	Nonsignificant	0.2894
4 dpa vs. 6 dpa	**	0.0072
4 dpa vs. 7 dpa	*	0.0254
4 dpa vs. 8 dpa	**	0.0033
4 dpa vs. 9 dpa	**	0.0066
4 dpa vs. 10 dpa	**	0.0014
5 dpa vs. 6 dpa	Nonsignificant	0.1323
5 dpa vs. 7 dpa	*	0.0285
5 dpa vs. 8 dpa	*	0.0182
5 dpa vs. 9 dpa	**	0.0064
5 dpa vs. 10 dpa	**	0.0025
6 dpa vs. 7 dpa	Nonsignificant	0.9758
6 dpa vs. 8 dpa	Nonsignificant	0.1658
6 dpa vs. 9 dpa	Nonsignificant	0.2537
6 dpa vs. 10 dpa	Nonsignificant	0.0508
7 dpa vs. 8 dpa	Nonsignificant	0.4118
7 dpa vs. 9 dpa	Nonsignificant	0.2558
7 dpa vs. 10 dpa	Nonsignificant	0.0984
8 dpa vs. 9 dpa	Nonsignificant	>0,9999
8 dpa vs. 10 dpa	Nonsignificant	0.3668
9 dpa vs. 10 dpa	Nonsignificant	0.4733

*, $P < 0.05$; **, $P < 0.01$.

Movie S1. Movie of a single osteolytic tubule of a *ctsk:DsRed* zebrafish following immunostaining for DsRed (magenta), highlighting DAPI-stained nuclei (blue). The represented osteolytic tubule is composed of 3 nuclei (arrows). The movie shows the different Z planes.

Movie S2. Movie of a magnified area of *SI Appendix*, Movie S1, showing a single nucleus (DAPI; blue) of an osteolytic tubule of a *ctsk:DsRed* zebrafish following immunostaining for DsRed (magenta). The movie shows the different Z planes.

SI Materials and Methods

Animals

All experiments were performed using adult (3-6 months old) or juvenile zebrafish (up to 3 weeks old). Animal husbandry followed standard conditions. All animal procedures followed institutional (CCMAR) guidelines, and the European and Portuguese legislation for animal experimentation and welfare (Directives 86/609/CEE and 2010/63/EU; Portaria 1005/92, 466/95 and 1131/97; Decreto-Lei 113/2013). Animal handling and experimentation were performed by qualified operators accredited by the Portuguese Direção-Geral de Alimentação e Veterinária (authorization no. 012769). All efforts were made to minimize pain, distress, and discomfort. Anesthesia was performed by incubating zebrafish in 0.6 mM tricaine solution (MS-222; Sigma-Aldrich, St. Louis, MO, USA). Euthanasia was performed using a lethal dose of anesthetic.

Caudal fin amputation

Amputation was performed 1-2 segments below the branchpoint of the most peripheral branching rays in anesthetized zebrafish. Upon amputation, zebrafish were transferred to isolated containers at a maximum density of 5.5 zebrafish/l. Water and light conditions were adjusted to match those of the rearing system, according to the standard conditions of zebrafish husbandry. All fin regeneration experiments took place at 33ºC, a standard temperature in regeneration studies (1-3).

Transcriptome analysis

Regenerated tissue was homogenized in solution D (4 M guanidinium thiocyanate, 25 mM sodium citrate pH 7.0, 0.5% N-laurosylsarcosine, 0.1 M 2-mercaptoethanol; all in DEPC-treated water) using a 20 G needle and total RNA was extracted through phenolic extraction as previously described (4). Briefly, 1 volume of phenol at pH 4.5 and 0.2 volume of chloroform/isoamyl alcohol mixture (49:1) was added to the homogenate (all chemicals from Sigma-Aldrich), and the mixture was inverted 2-3 times and cooled for 10 min on ice. The mixture was centrifuged at 10000 *g* for 15 min and the aqueous phase transferred to a new tube. RNA solution was further purified using 1 volume of chloroform/isoamyl alcohol mixture, as described above. Total RNA was precipitated by adding 1 volume of ice-cold 2-propanol (Sigma-Aldrich) to the aqueous phase and incubating the mixture for 24 hours at -80ºC. Precipitated RNA was pelleted (centrifugation at 12000 *g* for 10 min) and the supernatant removed. The RNA pellet was washed once with 75% ethanol and further centrifuged at 14000 *g* for 10 min. Ethanol was removed and the RNA pellet was air-dried at room temperature and resuspended in 30 µL of RNAse-free water (Sigma-Aldrich). All centrifugations were performed at 4ºC. Quantity and quality of the RNA were assessed using an Experion electrophoresis system (Bio-Rad, Hercules,

CA, USA) and samples with an RNA integrity number (RIN) > 8 were further processed for RNA-Seq.

The construction of cDNA libraries was carried out using the Illumina TruSeq Stranded mRNA Library Preparation kit. cDNA fragments were sequenced using the Illumina Hiseq 2500 platform with 100 bp paired-end sequencing reads.

Raw sequences were trimmed to generate high quality data using the CLC Genomics Workbench 9.0.1, as follows: quality trimming based on quality scores (0.01), ambiguity trimming (2 nucleotides) and length trimming (minimum of 30 bp). After quality and length trimming, base trim – to remove a specified number of bases at either 3' or 5' ends of the reads – was found unnecessary. For each original read, the regions of the sequence to be removed were determined independently of each type of trimming operation. Mapping of the reads was performed against the *Danio rerio* reference genome (assembly GRCz10) with length (minimum percentage of the total alignment length that must match the reference sequence at the selected similarity fraction) and similarity (minimum percentage identity between the aligned region of the read and the reference sequence) parameters set to 0.95. Gene expression was calculated based on the Reads per Kilobase of exon model per Million mapped reads (RPKM) approach (5).

Expression levels were calculated using the RPKM values from each sample independently. Differential expression was then calculated using a multi-factorial statistical analysis based on a negative binomial model that used a generalized linear model approach influenced by the multi-factorial EdgeR method (6). The differentially expressed genes were filtered using standard conditions (6, 7), i.e., a False Discovery Rate (FDR) *P* value <0.05 and a fold change >2 or <-2.

The quality of the produced data was ensured by evaluating the Phred quality score at each cycle (position in read; ensuring a minimum Phred score of 20). Further quality control was performed by principal component analysis (PCA), hierarchical clustering (considering Euclidean distance) and heat map analysis.

Gene ontology analysis was performed using PANTHER [Protein ANalysis THrough Evolutionary Relationships (8)] v16.0. For this analysis, Ensembl IDs of the genes upregulated at 3 dpa were used as input. Fisher's Exact test was performed to analyze for overrepresentation, using the Reactome pathway annotation set and the *Danio rerio* genome as a reference list. For the generation of the gene expression heat maps, Heatmapper (www.heatmapper.ca; University of Alberta) was used. Differential expression of selected genes was transformed to a Z-score per row and clustered using the average linkage clustering and the Euclidean distance measuring methods. The list of collagens, ECM regulators and other structural ECM components was retrieved from the zebrafish *in silico* matrisome (9).

Staining and immunohistochemistry

Mineral staining was performed in live animals following established protocols using alizarin red S (10) or calcein (11), both from Sigma-Aldrich, according to the need for combination with red or green fluorophores. Briefly, animals were incubated in system water containing 0.01% alizarin red or 0.2% calcein for up to 15 min and rinsed at least 3 times in clean system water. Imaging was performed in fins immediately after collection from euthanized zebrafish, or in anesthetized animals, depending on the need to track mineralization over time.

To assess bone-resorbing activity, the activity of tartrate resistant acid phosphatase (TRAP) was determined, as described (12). Briefly, fins were fixed in 4% PFA for 3 hours at room temperature, washed 5 times in PBT for 5 min and incubated in PBTx for 30 min. The samples were then incubated in TRAP buffer (50 mM sodium tartrate, 0.1 M acetic acid and 0.1 M sodium acetate; pH 4.4; all reagents were from Sigma-Aldrich) for approximately 20 min. The colorimetric assay was performed by incubating the samples in TRAP buffer containing 0.1 mg/ml Naphtol AS-MX phosphate and 0.3 mg/ml Fast Red Violet LB (Sigma-Aldrich). The samples were washed in 1× PBS for 5 min and cleared with 1.5% KOH for 5 min. The samples were then gradually transferred to 70% glycerol in 1× PBS and imaged under bright field or fluorescence microscopy.

Immunohistochemistry was performed immediately after staining for TRAP activity before transferring to glycerol. For that purpose, DsRed was immunostained in *ctsk:DsRed* zebrafish using a DsRed polyclonal primary antibody raised in rabbit (Living Colors DsRed, Cat. No. 632496; Takara, Bio Inc., Kusatsu, Shiga, Japan) and anti-rabbit Alexa Fluor 488 secondary antibody raised in goat (Invitrogen, Waltham, MA, USA). For detailed images of nuclei distribution within the OLTs, immunostaining for DsRed was performed similarly, but using anti-rabbit Alexa Fluor 568 secondary antibody raised in goat (Invitrogen). Nuclei were stained with DAPI (Sigma-Aldrich) diluted 1:5000 in 1× PBS for 30 min.

Ablation and drug treatments

For osteoblast ablation assays, wild-type and *sp7:*mCherry-NTR transgenic zebrafish were allowed to regenerate until 3 dpa. Zebrafish were then incubated in a Metronidazole (Mtz) solution, as previously described (13), for 24 hours. Mtz (Sigma-Aldrich) was freshly prepared in dimethylsulfoxid (DMSO, Sigma-Aldrich) and diluted in system water to a final concentration of 8.5 mM with 0.2% of DMSO. Control zebrafish were incubated in system water with 0.2 % DMSO alone. Both Mtz and vehicle-treated zebrafish were maintained for 24 hours in the dark to prevent Mtz degradation (14). Zebrafish were then rinsed twice to washout any traces of Mtz and returned to system water until 7 dpa. Mtz- and vehicle-treated zebrafish were anaesthetized and regenerates were collected and labelled with calcein to visualize the calcified bony rays.

Salmon calcitonin (Sigma-Aldrich) was prepared in 1× PBS and administered at 0.5, 5 and 50 µg/g through a single intraperitoneal injection at the time of fin amputation. Briefly, zebrafish were dried on absorbent paper and weighed immediately before the injection. A volume of 30 µl per gram of zebrafish was injected; injection solutions were adjusted to the desired concentrations accordingly. Control zebrafish were injected with the vehicle (1× PBS).

For the other drugs, zebrafish were continuously exposed by immersion in solutions prepared in system water, from the moment of fin amputation until the experimental endpoints. Dexamethasone (75 and 125 µM; Sigma-Aldrich), prednisolone (50 and 125 µM; Sigma-Aldrich) and all-trans retinoic acid (0.025 mg/l; Sigma-Aldrich) were prepared to achieve a working concentration of 0.1% DMSO; control zebrafish were exposed to 0.1% DMSO alone. Ibandronate (0.018 mg/g; Roche, Basel, Switzerland) was directly prepared in system water; control fish were placed in system water alone. 70% of the treatment solutions were renewed daily.

Microscopy and imaging

As mentioned above, imaging of adult zebrafish was performed under anesthesia or on collected fins, following animal euthanasia. For juvenile imaging, anesthetized zebrafish were placed directly under a Zeiss LSM800 Observer (Zeiss, Oberkochen, Germany) inverted confocal microscope and ZEN (Blue edition) software. For general histomorphometry, alizarin red stained fins were imaged under fluorescence conditions using a Leica MZ 7.5 fluorescence stereomicroscope (Leica Microsystems GmbH, Wetzlar, Germany), coupled to an F-View II camera controlled by the Cell^F v2.7 software (Olympus Soft Imaging Solutions GmbH, Münster, Germany), or using an MZ10F fluorescence stereomicroscope (Leica Microsystems GmbH), equipped with a Leica DFC7000T color camera. For bright field imaging, a SteREO Lumar.V12 (Zeiss) or a Nikon SMZ25 coupled with Nikon Digital Sight DS-Ri1 camera (Nikon, Minato City, Tokyo, Japan), were used. For detailed analyses, samples were imaged using a Zeiss LSM700 (Zeiss) or LSM800 inverted confocal microscope. For the osteoblast ablation studies, fins were imaged under a Zeiss Axio Observer z1 inverted microscope equipped with an Axiocam 506 monochromatic camera, using an EC Plan-Neofluar 5x 0.16NA air objective controlled by ZEN (Blue edition) software. Detailed images of nuclei were acquired using Cell Discoverer 7 with LSM900 (Zeiss) and ZEN (Blue edition).

Z projections of maximum intensity and orthogonal projections were performed using ImageJ v1.51n (Wayne Rasband, National Institutes of Health, Bethesda, MD, USA) or ZEN 3.1 (Blue edition). 3D reconstructions were performed using the Imaris (Bitplane) software. Fluorescence analysis of *sp7*:mCherry-NTR zebrafish was tracked over time, by determining the mean gray value of the regenerated area of dorsal ray #3, using ImageJ v1.51n.

Morphometry, quantifications and image analysis

The distance to branchpoint was determined by calculating the fraction of the length from the amputation plane to the branchpoint relative to the total mineralized length (from the amputation plane to the distal-most mineralized point). The mean of the relative distances to branchpoint of rays #2, 3, 4 and 5 (peripheral-most bifurcating rays) (12) from each lobe of each zebrafish were used in all comparative analyses. For the mineralization and branchpoint tracking analysis in single rays and comparative analysis based on ray length, ray #3 from the dorsal lobe of each zebrafish was measured. For quantification of TRAP activity, the number of rays displaying TRAP signal at the distal tip, coinciding with the branching area, was counted and calculated as percentage of the total number of rays within each fin. *shh:*GFP^{+} domains were evaluated by measuring their proximodistal length divided by the total mineralized ray length (from the amputation plane to the distal-most mineralized point).

Statistics

Statistical analyses were performed using Prism v9.3.1 (GraphPad Software Inc., La Jolla, CA, USA). Two-group comparisons were conducted using the unpaired, two-tailed Student's t-test when groups followed a normal distribution. Unpaired, two-tailed Student's t-test with Welch's correction was applied for comparisons using samples without normal distribution. Multiple one-factor comparisons were conducted using one-way ANOVA and Tukey's post hoc tests. For multiple one-factor comparisons of repeated measures, one-way ANOVA with Geisser-Greenhouse correction and Tukey's post hoc tests were used. For multiple one-factor comparisons using samples with significantly different standard deviations, Welch one-way ANOVA and Dunnett T3 post hoc tests were used. Multiple two-factor comparisons were conducted using two-way ANOVA (full model and repeated measures) with Geisser-Greenhouse correction and Šidák post hoc tests. Normality was tested through the Shapiro-Wilk's test. Bartlett's test was used to determine homogeneity of variances in one-factor multiple comparisons. Significance level was set to $\alpha=0.05$ for all tests.

SI Appendix References

1. J. Cardeira, *et al.*, Quantitative assessment of the regenerative and mineralogenic performances of the zebrafish caudal fin. *Sci. Rep.* **6**, 39191 (2016).

2. D. Oppedal, M. I. Goldsmith, A chemical screen to identify novel inhibitors of fin regeneration in zebrafish. *Zebrafish* **7**, 53–60 (2010).

3. A. Nechiporuk, M. T. Keating, A proliferation gradient between proximal and *msxb*-expressing distal blastema directs zebrafish fin regeneration. *Development* **129**, 2607–2617 (2002).

4. P. Chomczynski, N. Sacchi, The single-step method of RNA isolation by acid guanidinium thiocyanate-phenol-chloroform extraction: twenty-something years on. *Nat. Protoc.* **1**, 581–585 (2006).

5. A. Mortazavi, B. A. Williams, K. McCue, L. Schaeffer, B. Wold, Mapping and quantifying mammalian transcriptomes by RNA-Seq. *Nat. Methods* **5**, 621–628 (2008).

6. M. D. Robinson, D. J. McCarthy, G. K. Smyth, edgeR: a Bioconductor package for differential expression analysis of digital gene expression data. *Bioinformatics* **26**, 139–140 (2010).

7. K. Raza, A. Mishra, A novel anticlustering filtering algorithm for the prediction of genes as a drug target. *Am. J. Biomed. Eng.* **2**, 206–211 (2012).

8. H. Mi, S. Poudel, A. Muruganujan, J. T. Casagrande, P. D. Thomas, PANTHER version 10: expanded protein families and functions, and analysis tools. *Nucleic Acids Res.* **44**, D336–D342 (2016).

9. P. Nauroy, S. Hughes, A. Naba, F. Ruggiero, The *in-silico* zebrafish matrisome: a new tool to study extracellular matrix gene and protein functions. *Matrix Biol.* **65**, 5–13 (2018).

10. A. Bensimon-Brito, *et al*., Revisiting in vivo staining with alizarin red S - a valuable approach to analyse zebrafish skeletal mineralization during development and regeneration. *BMC Dev. Biol.* **16**, 2 (2016).

11. S. J. Du, V. Frenkel, G. Kindschi, Y. Zohar, Visualizing normal and defective bone development in zebrafish embryos using the fluorescent chromophore calcein. *Dev. Biol.* **238**, 239–246 (2001).

12. N. Blum, G. Begemann, Retinoic acid signaling spatially restricts osteoblasts and controls ray-interray organization during zebrafish fin regeneration. *Development* **142**, 2888–2893 (2015).

13. S. P. Singh, J. E. Holdway, K. D. Poss, Regeneration of amputated zebrafish fin rays from de novo osteoblasts. *Dev. Cell* **22**, 879–886 (2012).

14. S. Curado, D. Y. R. Stainier, R. M. Anderson, Nitroreductase-mediated cell/tissue ablation in zebrafish: a spatially and temporally controlled ablation method with applications in developmental and regeneration studies. *Nat. Protoc.* **3**, 948–54 (2008).